BIOCHEMISTRY
including biophysical chemistry & molecular biology
Article

Biochemistry **2011,** *50,* 981–988 981
DOI: 10.1021/bi101549n

Thermal Induction of an Alternatively Folded State in Human IgG-Fc[†]

Daniel Kanmert,[‡] Ann-Christin Brorsson,[§] Bengt-Harald Jonsson,[§] and Karin Enander*[,‡]

[‡]*Division of Molecular Physics, Department of Physics, Chemistry and Biology, Linköping University, SE-581 83 Linköping, Sweden, and* [§]*Division of Molecular Biotechnology, Department of Physics, Chemistry and Biology, Linköping University, SE-581 83 Linköping, Sweden*

Received September 24, 2010; Revised Manuscript Received January 4, 2011

ABSTRACT: We report the formation of a non-native, folded state of human IgG4-Fc induced by a high temperature at neutral pH and at a physiological salt concentration. This structure is similar to the molten globule state in that it displays a high degree of secondary structure content and surface-exposed hydrophobic residues. However, it is highly resistant to chemical denaturation. The thermally induced state of human IgG4-Fc is thus associated with typical properties of the so-called alternatively folded state previously described for murine IgG, IgG-Fab, and individual antibody domains (V_L, V_H, C_H1, and C_H3) under acidic conditions in the presence of anions. Like some of these molecules, human IgG4-Fc in its alternative fold exists as a mixture of different oligomeric structures, dominated by an equilibrium between monomeric and heptameric species. Heating further induces the formation of fibrous structures in the micrometer range.

Many proteins can form folded, non-native structures with lifetimes sufficiently long to make them amenable for characterization. Most intensively studied among these is the molten globule state (*1*), an ensemble of rapidly interconverting conformations that is observed as a folding intermediate and that can be induced from the native structure via a change in temperature or pH or by exposure to relatively low concentrations of a denaturant. The molten globule state is associated with an average degree of secondary structure similar to that of the native state, but hydrophobic residues are solvent-accessible and tertiary contacts poor, resulting in a less compact structure. Moreover, the molten globule is only marginally stable against denaturants and unfolds noncooperatively.

Murine immunoglobulin G (IgG)[1] forms a folded structure upon acidification that is distinct from both the native conformation and the molten globule state (*2*, *3*). This so-called alternatively folded state is associated with a high degree of secondary structure and solvent-exposed hydrophobic residues. It further displays an apparently higher stability toward chemical denaturation compared to the native state and unfolds in cooperative transitions. Similar results have been obtained with the IgG-Fab fragment, provided that the intermolecular disulfide bridge between the light chain and the Fd chain is intact (*4*, *5*), and with individual antibody domains (V_L, V_H, C_H1, and C_H3), where the conformational changes at secondary and tertiary levels induce the formation of oligomers of ∼5−40 monomeric units (*6*, *7*).

In this study, we present an alternatively folded state of hIgG4-Fc induced by a high temperature at neutral pH and at a physiological salt concentration. Upon thermal denaturation, there is an irreversible structural rearrangement reflected at secondary, tertiary, and quaternary levels. Compared to the native state, the alternatively folded state of hIgG4-Fc displays an increased level of exposure of hydrophobic residues and an apparently increased stability toward chemical denaturation, indicating that unfolding is kinetically controlled. It also induces the formation of oligomeric structures and micrometer-sized fibers.

MATERIALS AND METHODS

Gene Cloning and Transformation into Pichia pastoris. *Escherichia coli* strain TOP10 (Invitrogen, Carlsbad, CA) was used as a plasmid host throughout the cloning procedures. The genes encoding the Fc fragment (hinge-C_H2-C_H3) of hIgG1, hIgG2, hIgG3, and hIgG4 were isolated from the following cDNA clones using standard molecular biology procedures: *hIgG1-Fc*, FL22942 (Genecopoiea, Rockville, MD); *hIgG2-Fc*, 10467566; *hIgG3-Fc*, 912466; and *hIgG4-Fc*, 22866 (ATCC, Manassas, VA). The gene fragments were inserted into plasmid pGAPZα (Invitrogen), and the final constructs were designated pGAPZα-*hIgG1-Fc*, pGAPZα-*hIgG2-Fc*, pGAPZα-*hIgG3-Fc*, and pGAPZα-*hIgG4*-Fc. The identities of the constructs were verified by sequencing. Ten micrograms of each plasmid was linearized using AvrII and transformed into *P. pastoris* GS115 (Invitrogen) by electroporation. The transformation reaction mixtures were plated on YPDS (1% yeast extract, 2% peptone, 2% D-glucose, and 1 M sorbitol) agar containing 100 μg/mL zeocin as a selection marker, and colonies were purified by replica plating three times. At least 20 separate 10 mL YPD (1% yeast

[†]This work was supported by the Swedish Foundation for Strategic Research (SSF) through the NanoSense and Biomics programs.

*To whom correspondence should be addressed. Telephone: +46 13 282359. Fax: +46 13 137568. E-mail: karen@ifm.liu.se.

[1]Abbreviations: ANS, 8-anilino-1-naphthalenesulfonic acid; AUC, analytical ultracentrifugation; CD, circular dichroism; DSC, differential scanning calorimetry; ELISA, enzyme-linked immunosorbent assay; GdmHCl, guanidinium hydrochloride; hIgG4-Fc, human immunoglobulin G crystallizable fragment of subclass 4; IgG, immunoglobulin G; IgG-C_H3, C_H3 domain of immunoglobulin G; IgG-Fab, immunoglobulin G antigen binding fragment; MALDI-TOF, matrix-assisted laser desorption ionization time-of-flight; PBS, phosphate-buffered saline; RF, rheumatoid factor; SDS−PAGE, sodium dodecyl sulfate−polyacrylamide gel electrophoresis; SPR, surface plasmon resonance; TEM, transmission electron microscopy; UV, ultraviolet; YPD, yeast extract peptone dextrose medium; YPDS, yeast extract peptone dextrose medium with sorbitol.

Published on Web 01/24/2011

extract, 2% peptone, and 2% D-glucose) medium aliquots containing 100 μg/mL zeocin were inoculated with single colonies from selection plates and allowed to grow for 48 h. The cells were removed by centrifugation at 5000*g* for 15 min at 4 °C, and the presence of hIgG-Fc in the supernatants was confirmed by dot blotting using a rabbit anti-human IgG as primary antibody and a secondary swine anti-rabbit IgG antibody conjugated to horseradish peroxidase for revelation. Clones expressing hIgG-Fc of each subclass were isolated and designated GS115-*hIgG1-Fc*, GS115-*hIgG2-Fc*, GS115-*hIgG3-Fc*, and GS115-*hIgG4-Fc*. Ten micrograms of plasmid pGlycoSwitch-M5 (plasmid collection accession no. 4924, BCCM/LMBP, Zwijnaarde, Belgium) was linearized using BstBI and transformed into the *P. pastoris* clones by electroporation. Colonies were purified by replica plating three times using 300 μg/mL blasticidin as a selection marker. The final clones were designated GS115M5-*hIgG1-Fc*, GS115M5-*hIgG2-Fc*, GS115M5-*hIgG3-Fc*, and GS115M5-*hIgG4-Fc*.

Protein Expression and Purification. A 20 mL YPD preculture was diluted 50 times in 1 L of YPD in a baffled shake flask. Protein expression was allowed to continue for 72 h with shaking at 30 °C. Cells were removed from the culture by centrifugation at 3000*g* for 30 min at 4 °C. The supernatant was passed through a 0.45 μm filter, and the pH was adjusted to 8.2. The sample was applied on a column containing 1 mL of Protein G Sepharose 4 Fast Flow (GE Healthcare, Uppsala, Sweden) at a flow rate of 2 mL/min. The gel was washed with 10 column volumes of 50 mM sodium phosphate and 100 mM NaCl (pH 8.2) and 10 column volumes of 50 mM sodium phosphate and 500 mM NaCl (pH 8.2). The bound protein was eluted using 0.1 M glycine-HCl (pH 2.6). The eluate was collected in 0.8 mL fractions into 0.2 mL of 1 M Tris-HCl (pH 8.0). The pooled fractions containing protein were dialyzed against PBS (10 mM sodium phosphate, 140 mM NaCl, and 2.7 mM KCl) at pH 7.4. Protein purity was assessed by SDS−PAGE. Protein concentrations were determined from the absorbance at 280 nm, using the calculated extinction coefficients of 71570 M^{-1} cm^{-1} (hIgG1-Fc), 65860 M^{-1} cm^{-1} (hIgG2-Fc), 66610 M^{-1} cm^{-1} (hIgG3-Fc), and 71570 M^{-1} cm^{-1} (hIgG4-Fc).

CD Spectroscopy. Data were recorded on a Chirascan CD spectrometer (Applied Photophysics Ltd., Surrey, United Kingdom) in 0.1 and 0.4 cm path length quartz cuvettes for far- and near-UV regions, respectively, and at a protein concentration of 5 μM in PBS (pH 7.4). The change in ellipticity at 216 nm was monitored every 0.1 °C during a linear temperature ramping (1 °C/min) from 5 to 95 °C for hIgG4-Fc. Full spectra between 200 and 260 nm were recorded every 0.5 nm with an integration time of 0.5 s (20 consecutive scans) at 25 °C, at 75 °C, and after re-equilibration at 25 °C for hIgG-Fc (subclasses 1−4). Full spectra were also recorded between 240 and 340 nm for hIgG4-Fc. For the temperature-jump experiment, a room-tempered sample of hIgG4-Fc was diluted (final concentration of 5 μM) directly into buffer equilibrated at 75 °C. Ten consecutive far-UV scans (one scan per minute) were recorded immediately, smoothed, and presented individually. A buffer spectrum [PBS (pH 7.4)] was used for reference subtraction. All measurements were performed three times, and representative results are shown.

Intrinsic Tryptophan Fluorescence. Data were recorded on a Fluoromax-4 spectrofluorometer (Horiba Jobin-Yvon, Edison, NJ) in a 1 cm path length quartz cuvette and at a protein concentration of 5 μM in PBS (pH 7.4). The excitation wavelength was 295 nm, and the emission spectra were recorded in the interval of 310−450 nm (three consecutive scans) with entrance and exit slits set to 5 nm, at 25 °C, at 75 °C, and after re-equilibration at 25 °C. The change in tryptophan fluorescence was also monitored every 2 °C in a stepped temperature increase (2 °C steps with equilibration for 5 min at each step). Data were fitted with nonlinear least-squares analysis to a logistic function. A buffer spectrum [PBS (pH 7.4)] was used for reference subtraction. All measurements were performed three times, and representative results are shown.

ANS Binding Analysis. Data were recorded on a Fluoromax-4 spectrofluorometer (Horiba Jobin-Yvon) in a 1 cm path length quartz cuvette and at a protein concentration of 5 μM in PBS (pH 7.4). ANS was added to a final concentration of 100 μM just prior to the measurement. The excitation wavelength was 360 nm, and the emission spectra were recorded in the interval of 400−650 nm (three consecutive scans) with entrance and exit slits set to 5 nm, at 25 °C, at 75 °C, and after re-equilibration at 25 °C. The ANS fluorescence at 485 nm was monitored in a stepped temperature ramping, with equilibration for 5 min at each step. A spectrum of ANS in PBS (pH 7.4) was used for reference subtraction. All measurements were performed three times, and representative results are shown.

Limited Proteolysis. Samples of native and heat-treated (10 min at 75 °C) hIgG4-Fc at 5 μM in 10 mM sodium acetate (pH 4.4) were incubated with trypsin (1.25 μg/mL) (Sigma-Aldrich, St. Louis, MO) at 37 °C. The proteolysis reactions were quenched after 0.5, 1, or 2 h by the addition of acetic acid to a final concentration of 0.5% (w/w). Autoproteolysis controls were included by incubation of trypsin alone. The peptide fragments were identified by MALDI-TOF mass spectrometry on a Voyager workstation (Applied Biosystems, Foster City, CA).

Stability Analysis. The stability toward GdmHCl unfolding was monitored by recording changes in the intrinsic tryptophan fluorescence. The protein concentration was 1 μM in PBS (pH 7.4). Native (25 °C) or heat-treated (10 min at 75 °C) protein was incubated with GdmHCl at different concentrations (0−6 M) overnight. GdmHCl concentrations were determined refractometrically (*8*). Data were recorded at 25 °C on a Fluoromax-4 spectrofluorometer (Horiba Jobin-Yvon) in a 1 cm path length quartz cuvette. The excitation wavelength was 295 nm, and the emission spectra were recorded in the interval of 310−450 nm (three consecutive scans) with entrance and exit slits set to 5 nm. Measurements were performed three times. For each sample, the intensity at 355 nm was divided by the intensity at 338 or 343 nm for native or heat-treated protein, respectively, to give r. The fraction unfolded y was obtained from

$$y = \frac{r - r(\mathrm{N})}{r(\mathrm{U}) - r(\mathrm{N})} \quad (1)$$

where r(N) and r(U) are the intensity ratios at 0 and 6 M GdmHCl, respectively. To obtain stability parameters, data were fitted with nonlinear least-squares analysis to the following equation:

$$y = \frac{y(\mathrm{N}) + y(\mathrm{U})A}{1 + A}; \quad A = e^{m[\mathrm{GdmHCl}] - \Delta G^{H_2O}/RT} \quad (2)$$

where y(N) and y(U) represent the fractions unfolded at 0 and 6 M GdmHCl, respectively, m is a constant corresponding to the exposure of the protein surface upon denaturation, ΔG^{H_2O} is the free energy of unfolding in water, R is the gas constant, and T is the temperature in kelvin. When the data for the unfolding of the heat-treated protein were fitted, two data points corresponding to

the lowest denaturant concentrations were omitted. The stability toward GdmHCl unfolding of native hIgG4-Fc was also monitored by following changes in the negative ellipticity at 228 nm using CD spectroscopy.

AUC Analysis. Sedimentation equilibrium data were obtained on a Beckman Coulter XL-1 analytical ultracentrifuge (Beckman Coulter, Brea, CA) equipped with an An-50 Ti rotor with a six-well centerpiece with a 1.2 cm path length. Experiments with native (25 °C) and heat-treated (75 °C for 10 min) hIgG4-Fc [5 μM in PBS (pH 7.4)] were conducted at 25 °C and 4000, 6000, 8000, 12000, and 18000 rpm. Background was subtracted for each sample well using data from PBS (pH 7.4). The sedimentation properties were analyzed by using the self-association model in the Beckman software package.

TEM Imaging. Cupper grids were charged with UV light for 5 min just before use. Ten microliters of 5 μM heat-treated (75 °C for 20 h) hIgG4-Fc in PBS (pH 7.4) was adsorbed on the grids for 2 min. Grids were then blotted dry, washed with 2 × 10 μL of ddH_2O, blotted dry, and counterstained using 10 μL of 2% (w/v) uranyl acetate in ddH_2O for 2 min. They were then blotted dry and allowed to air-dry. Micrographs were collected using a Jeol 1230 transmission electron microscope (Jeol Ltd., Tokyo, Japan) equipped with an ORIUS SC1000 CCD camera.

RESULTS

The genes encoding hIgG-Fc (subclasses 1−4) were successfully inserted in frame with the GAP promotor in the pGAPZα plasmid, and the inserts were verified by DNA sequencing. *P. pastoris* transformants were isolated through replica plating under antibiotic selection. The protein was expressed directly into the cultivation medium. Protein purity after affinity purification was determined to >95% by SDS−PAGE.

CD Spectroscopy. The Fc fragment of IgG antibodies has a molecular mass of ~60 kDa. The polypeptide chain comprising the C_H2 and C_H3 domains folds into β-barrel structures consisting of antiparallel β-sheets packed tightly against each other. The far-UV CD spectrum of hIgG4-Fc at 25 °C (Figure 1A, solid line) reveals a minimum at 216 nm that is characteristic of β-sheet proteins (*9*). The minimum at 228 nm is due to contributions from aromatic side chains and/or disulfide bonds (*10*). When the ellipticity at 216 nm during linear temperature ramping in the interval of 5−95 °C is monitored (Figure 1B), there is a dramatic increase in negative ellipticity between 60 and 75 °C (T_m = 67 °C), indicating a cooperative structural rearrangement at a secondary level that is not equivalent with the formation of a random coil. To investigate whether the transition from the native fold to the structural state induced by heating is a reversible process, full far-UV CD spectra were recorded both at 75 °C (Figure 1A, dashed line) and after re-equilibration of the protein sample at 25 °C (Figure 1A, dotted line marked 4). Compared to the spectrum recorded at 75 °C, that of the re-equilibrated sample shows an only slight decrease in negative ellipticity, and the overall shape of the curve is unchanged. Thus, the protein does not return to its native fold upon cooling, implying an irreversible structural change induced by heating to 75 °C. To investigate if the structural rearrangement observed with hIgG4-Fc is a property common to all subclasses of hIgG-Fc, far-UV CD spectra of hIgG1-Fc, hIgG2-Fc, and hIgG3-Fc were recorded after heating (75 °C) and after re-equilibration at 25 °C. For the sake of clarity, only spectra recorded after re-equilibration at 25 °C are shown (Figure 1A, dotted lines marked 1−3), because the spectra of native hIgG-Fc of subclasses 1−3 are almost identical to that of hIgG4-Fc. Also, thermal denaturation is irreversible in all cases; i.e., the same relative decrease in negative ellipticity when the samples are re-equilibrated at 25 °C after heating is observed for all proteins. Spectra from the four heat-treated hIgG-Fc samples are clearly different. With hIgG1-Fc, there is no well-defined minimum of the spectrum, while there is a pronounced blue shift, compared to that of hIgG4-Fc, of the minima observed with hIgG2-Fc and hIgG3-Fc, indicating a substantial contribution of random coil to the structure in these molecules. Evidently, minor differences in sequence and native structure have a significant impact on the thermally induced state in hIgG-Fc.

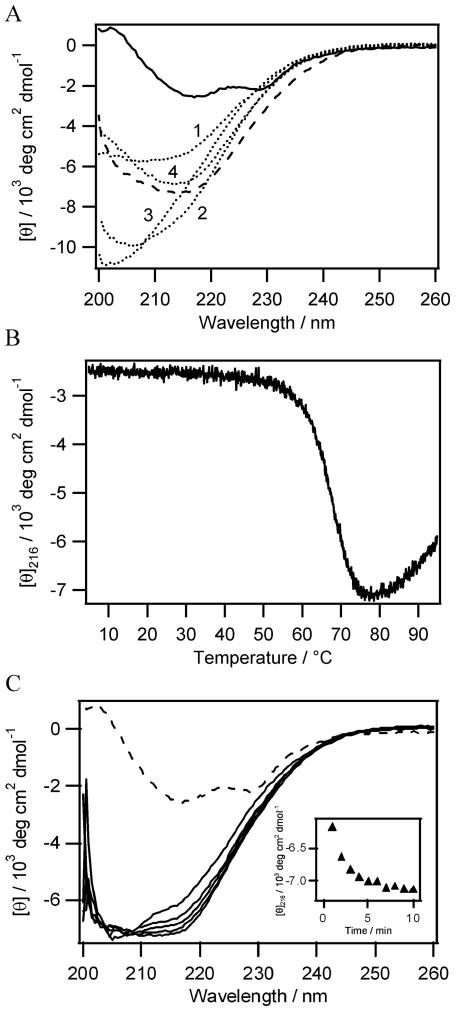

FIGURE 1: Far-UV CD analysis of hIgG4-Fc (5 μM). (A) Spectra were recorded at 25 °C (—), after equilibration at 75 °C (---), and after re-equilibration at 25 °C (···, marked 4). Spectra for hIgG-Fc of subclasses 1−3 after re-equilibration at 25 °C are also shown (numbers relate to the hIgG-Fc subclass). (B) Mean residue ellipticity at 216 nm monitored during temperature ramping. (C) Spectra recorded after 1, 2, 3, 6, and 10 min (—, from top to bottom) at 75 °C. A spectrum of native protein is also shown (---). The inset shows the mean residue ellipticity at 216 nm monitored for the first 10 min of equilibration.

Temperature-jump analysis of hIgG4-Fc revealed that the major part of the structural conversion occurs within the first minute of heating (Figure 1C, main graph). Some additional decrease in the negative ellipticity at 216 nm suggests minor structural changes on the 1−10 min time scale (Figure 1C, inset), but clearly, there are no indications of on-pathway intermediates

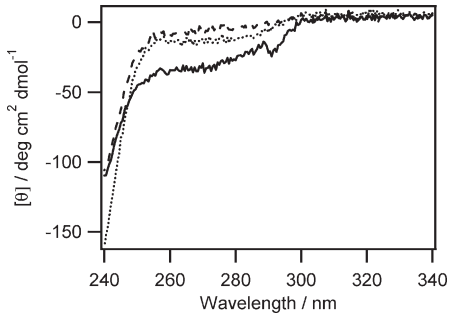

FIGURE 2: Near-UV CD analysis of hIgG4-Fc (5 μM). Spectra were recorded at 25 °C (—), after equilibration at 75 °C (---), and after re-equilibration at 25 °C (· · ·).

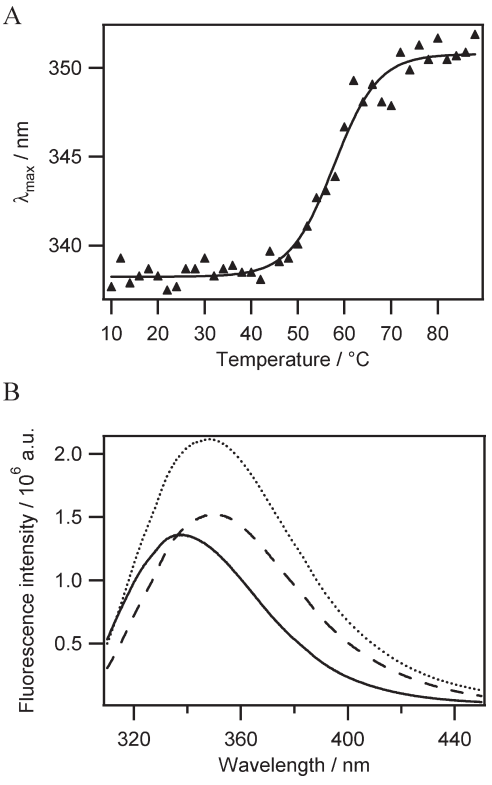

FIGURE 3: Intrinsic tryptophan fluorescence from hIgG4-Fc (5 μM). (A) Wavelength of maximal emission intensity monitored during temperature ramping. The solid line represents a least-squares fit. (B) Fluorescence emission spectra recorded at 25 °C (—), after equilibration at 75 °C (---), and after re-equilibration at 25 °C (· · ·).

within this window of observation. No further changes in the spectra were found beyond 10 min (not shown). Thus, if intermediates are formed, they are short-lived.

The near-UV CD scan is often used to indicate changes in the tertiary structure of a protein. The near-UV CD signal of native hIgG4-Fc contains a broad and shallow trough (250−300 nm) devoid of distinct bands (Figure 2, solid line), which precludes detailed conclusions regarding tertiary structure rearrangement. However, the disappearance of this trough upon heating (Figure 2, dashed line) and subsequent cooling (Figure 2, dotted line) indicates loss of structure.

Intrinsic Tryptophan Fluorescence. Because of the large number of tryptophan residues (eight) evenly distributed throughout the hIgG4-Fc molecule, monitoring the changes in intrinsic tryptophan fluorescence is a sensitive method for following global alterations in tertiary structure in this protein.

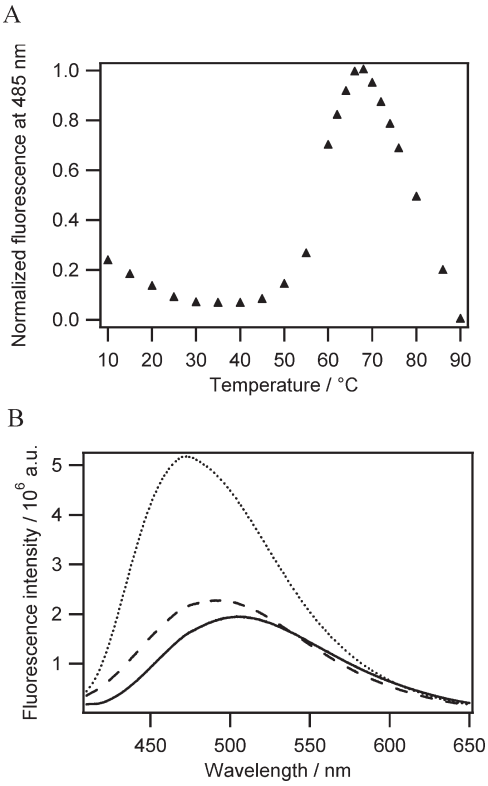

FIGURE 4: ANS fluorescence from a sample containing 5 μM hIgG4-Fc and 100 μM ANS. (A) Emission intensity at 485 nm monitored during temperature ramping. (B) Spectra recorded at 25 °C (—), after equilibration at 75 °C (---), and after re-equilibration at 25 °C (· · ·).

Thermal denaturation of hIgG4-Fc results in a red shift of the wavelength at maximal intensity (λ_{max}) from ~338 to ~352 nm (Figure 3A), and T_m, obtained from fitting to a two-state model, is 59 °C. Full emission scans (Figure 3B) were recorded at 25 °C, at 75 °C, and after re-equilibration of the heated protein sample at 25 °C. The λ_{max} of the re-equilibrated sample is 348 nm, and its emission intensity increases substantially compared to that recorded at 75 °C.

ANS Binding Analysis. To investigate whether heating of hIgG4-Fc induces a structural change that is associated with hydrophobic patches being exposed on the protein surface, the probe ANS was added to a protein sample and the ANS fluorescence emission was monitored during a stepped temperature ramping experiment (Figure 4A). When ANS binds to hydrophobic regions in proteins, its emission intensity increases and λ_{max} exhibits a blue shift of ~40 nm from 520 nm in water (*11*). At ~50 °C, the ANS fluorescence at 485 nm starts to increase and reaches a maximum at 68 °C. At higher temperatures, the emission intensity decreases. Full emission scans (Figure 4B) reveal that when the heated sample is re-equilibrated at 25 °C, λ_{max} shifts to the blue slightly while the intensity becomes significantly higher.

Limited Proteolysis. To determine which parts of the hIgG4-Fc molecule that are involved in heat-induced structural rearrangements, limited proteolysis by trypsin was performed. The obtained cleavage patterns (Figure 5) show that heating increases the number of accessible cleavage sites. The numbers of fragments appearing after cleavage for 0.5, 1, and 2 h are two, five, and five (native protein) and three, four, and seven (heat-treated protein), respectively. Most notably, the N-terminal fragment corresponding to residues 223−240 (residue numbers adopted

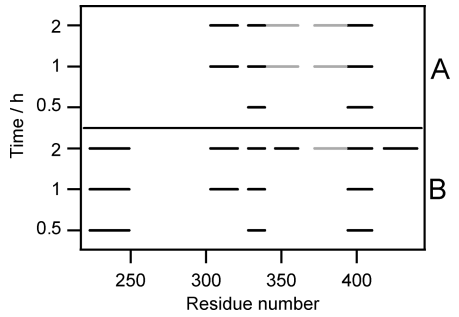

FIGURE 5: Cleavage patterns after limited trypsin proteolysis of hIgG4-Fc. Panels A and B show peptide fragments identified by MALDI-TOF mass spectrometry after proteolysis for 0.5, 1, and 2 h of native and heat-treated protein, respectively. Different color intensities (black and gray) are used to visually separate fragments in cases where they are immediately adjacent. Residue numbers are adopted from the full hIgG4 heavy chain.

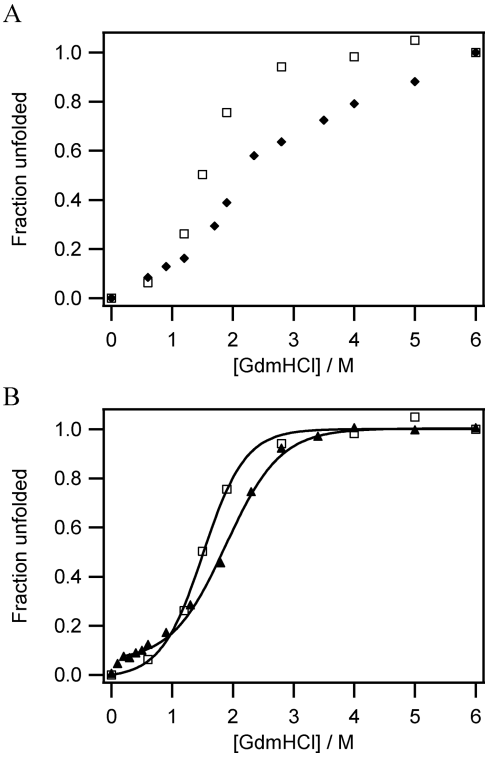

FIGURE 6: Stability of hIgG4-Fc toward GdmHCl-induced unfolding. (A) Unfolding transitions of native protein at 25 °C monitored with far-UV CD (◆) and intrinsic tryptophan fluorescence (□). (B) Unfolding transitions monitored with intrinsic tryptophan fluorescence of the native protein at 25 °C (□, same data set as in panel A) and heat-treated protein (75 °C for 10 min) after re-equilibration at 25 °C (▲). Data points represent mean values from three measurements, and solid lines represent least-squares fits.

from the full hIgG4 heavy chain), which emanates from a largely buried area in the native protein, appears already after 0.5 h in the heat-treated protein. Other parts showing differences in cleavage accessibility include residues 340−393 and the C-terminus (residues 416−443).

Stability toward GdmHCl Denaturation. The global unfolding of native and heat-treated hIgG4-Fc was analyzed by monitoring the intrinsic fluorescence from the eight evenly distributed tryptophan residues in the presence of increasing concentrations of GdmHCl. To address the complexity of unfolding of the native protein, its far-UV CD signal at 228 nm was also monitored. The unfolding curves of the native protein recorded by intrinsic fluorescence and far-UV CD did not coincide (Figure 6A), indicating that unfolding of native hIgG4-Fc cannot be described as a two-state process.

An equation describing equilibrium unfolding was useful for obtaining stability parameters from the unfolding curves of the native and heat-treated protein measured by intrinsic fluorescence (Figure 6B). C_m values of 1.5 ± 0.02 and 1.9 ± 0.03 M GdmHCl, ΔG values in water of 2.6 ± 0.1 and 2.6 ± 0.2 kcal/mol, and m values of 1.8 ± 0.1 and 1.4 ± 0.1 kcal mol^{-1} M^{-1} were determined for the native and heat-treated proteins, respectively (mean from three measurements in each case). The heat-treated protein is apparently more stable, deduced from the higher C_m value, but unfolds less cooperatively than the native protein (Figure 6B). Importantly, it is obvious that the system is not at thermal equilibrium, because the unfolding of the protein depends on its initial structural state [i.e., heat-treated hIgG4-Fc is apparently more stable than the native protein (Figure 6B)] and because transitions are not reversible (not shown). Therefore, unfolding is under kinetic control, and the parameter values obtained from fitting are not true thermodynamic descriptors of the unfolding process. However, they can be used as indicators to describe differences between the two structural variants of the protein.

Size Determination. To investigate whether thermally induced changes of hIgG4-Fc at the secondary and tertiary levels are accompanied by changes in quaternary structure, AUC was employed. It was confirmed that the native protein is a dimer with a molecular mass of ~60 kDa. In contrast, heat-treated hIgG4-Fc forms higher-order assemblies, dominated by an equilibrium between monomeric and heptameric species (Figure S1 of the Supporting Information). At the concentration used (5 μM), 20% of the protein is heptameric.

TEM Imaging. TEM was used for further analysis of changes in the quaternary structure upon thermal treatment. Micrographs of hIgG4-Fc recorded after incubation for 20 h at 75 °C reveal the presence of fibrous structures in the micrometer range (Figure 7).

DISCUSSION

Temperature-induced structural changes leading to non-native folded conformations have been reported for a number of all-β-sheet proteins. Cell adhesion protein CD2-1, which belongs to the immunoglobulin family, rearranges reversibly into a non-native helical conformation when heated above 68 °C in PBS (pH 7.3) (*12*). Similarly, thermal denaturation of murine tumor necrosis factor-α irreversibly results in a non-native, α-helix-containing structure (T_m = 66 °C) (*13*), while the soybean Kunitz trypsin inhibitor forms a molten state above 65 °C that refolds into the native state upon cooling (*14*).

The different structural states of IgG domains have been extensively studied in the quest for a general understanding of the folding pathways of all-β-sheet proteins [see the recent review by Feige et al. (*15*) and references cited therein]. Also, the advent of therapeutic antibodies has recently renewed the interest in studying the stability of IgG (*16*). IgG-Fc is a dimeric β-sheet protein stabilized by interactions between the C_H3 domains and between the N-linked oligosaccharides in the C_H2 domains. The two monomers are connected with disulfide bonds in the hinge region. In several reports, DSC experiments with hIgG-Fc have revealed two transitions attributed to thermal unfolding of C_H2

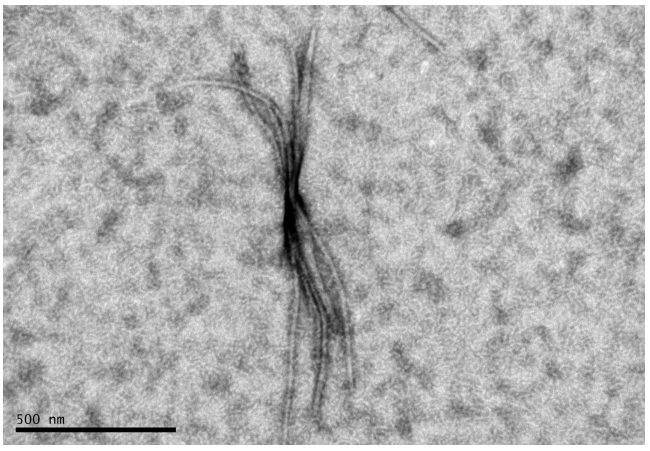

FIGURE 7: Transmission electron micrograph of fibers formed from hIgG4-Fc after incubation of the protein sample (5 μM) for 20 h at 75 °C.

($T_m \sim 70-72$ °C) and C_H3 ($T_m \sim 82-84$ °C) (*16*−*19*), and it has been proposed that hIgG-Fc forms a molten globule state during thermal denaturation (*20*). However, the work presented here unambiguously shows that disruption of the native structure of hIgG4-Fc during heating results in a folded conformation with properties that are in part different from those associated with the classical molten globule state. Rather, it is very similar to the so-called alternatively folded state that has been described for murine IgG, IgG-Fab, and some isolated IgG domains under acidic conditions (*2*−*4*, *6*, *7*).

hIgG4-Fc displays a typical far-UV CD spectrum of a β-sheet protein at room temperature and pH 7.4 with a dip at 216 nm (Figure 1A). The significant increase in the negative ellipticity during temperature ramping, accompanied by a slight shift of the dip to 214 nm, can most straightforwardly be interpreted as an increase in the β-sheet secondary structure content, possibly in combination with some contribution from the random coil state. However, other all-β-proteins with very similar spectra have been proposed to contain some α-helical structure as well (*6*, *13*). The T_m (67 °C) reasonably well agrees with the temperature for the first DSC transition for hIgG1-Fc reported in the literature (*16*−*19*) and also coincides with the melting transition temperature of many other all-β-sheet proteins (*12*−*14*). Above 75 °C, the negative ellipticity again decreases, indicating further structural rearrangement. The conversion of hIgG4-Fc from the native state to the structure at 75 °C is a fast and irreversible process, as is evident from temperature-jump experiments (Figure 1C) and the far-UV CD spectrum of the heat-treated protein after re-equilibration at 25 °C (Figure 1A).

The red shift of the intrinsic tryptophan fluorescence above 50 °C (Figure 3A) reveals that a less compact protein conformation is being formed upon heating where tryptophan residues are accessed by solvent molecules. As expected, the tertiary structure of the protein is affected before the secondary structure elements are rearranged. This is illustrated by the lower transition temperature observed upon monitoring of tryptophan accessibility (59 °C) compared to that observed when monitoring changes in the secondary structure in far-UV CD (67 °C). Near-UV CD data (Figure 2) further confirm the loss of tertiary structure upon thermal denaturation.

When the protein is heated, the fluorescence signal from the tryptophans is slightly enhanced compared to that observed at room temperature (Figure 3B). Tryptophan residues in native proteins are often quenched internally by local contacts with either disulfide bridges or each other (*21*). In hIgG4-Fc, four of the eight tryptophan residues are in the proximity of intramolecular disulfide bridges (*22*). It is likely that the less compact structure induced upon heating is associated with physical separation of these groups, followed by a reduced level of quenching. However, at 75 °C, intermolecular quenching may be substantial because of the higher mobility of the molecules at elevated temperatures. When the protein is re-equilibrated at 25 °C, this effect disappears. Alternatively, cooling may induce a structural state with a different tertiary structure compared to that prevailing at 75 °C, where the level of intramolecular quenching is even more reduced.

The ANS binding experiment shows that the heat-induced structural rearrangement of hIgG4-Fc is accompanied by the formation of hydrophobic patches on the protein surface. Intermolecular interactions between these patches most likely drive the formation of the oligomeric structures evident from AUC data of the heat-treated protein after re-equilibration to 25 °C (discussed below). The ANS fluorescence peaks at 68 °C, followed by a pronounced decrease at higher temperatures (Figure 4A). This could possibly be explained by significantly larger but still soluble aggregates being formed above 68 °C, shielding the hydrophobic patches from the solvent and preventing ANS from binding. This effect would be even more pronounced if the affinity between the protein and ANS is reduced at these elevated temperatures. When the heat-treated protein is re-equilibrated at 25 °C, the intensity of the ANS emission is significantly increased (Figure 4B). A possible explanation for this observation is that more hydrophobic patches are exposed upon cooling, as a result of the fact either that the oligomers formed at 75 °C interact with lower affinity at reduced temperatures or that a structural state is formed, distinct from that at 75 °C, that may be associated with a higher surface concentration of hydrophobic patches. Again, if the affinity between the protein and ANS is temperature-dependent and increased upon cooling, this would also contribute. A lower affinity between oligomers upon re-equilibration at room temperature may also be an additional explanation for the fact that the tryptophan fluorescence increases upon cooling (Figure 3B), because this may reduce the level of intermolecular quenching.

Structural rearrangements at secondary and tertiary levels resulted in distinct differences in the accessibility to proteolysis for native and heat-treated hIgG4-Fc (Figure 5). Inspection of the X-ray crystal structure of native hIgG4-Fc (*22*) reveals that the protein fold is globally altered upon heating; i.e., rearrangement involves both C_H2 and C_H3 domains, and β-strands forming part of the dimer interface are affected as well as those being exposed to the ambient. The N-terminal β-strand (in C_H2) is shielded from the solvent in the native dimer, but thermally induced rearrangements result in an increased level of exposure. Also, the C-terminus (in C_H3) becomes more accessible to cleavage after heating. In contrast, residues 340−393 (in C_H3) seem to be buried to a larger extent in the heated than in the native protein.

Spectroscopic data from hIgG4-Fc at elevated temperatures show many similarities to corresponding data obtained with the acid-induced alternatively folded states of murine IgG, IgG-Fab, and IgG-C_H3 (*2*, *4*, *6*, *7*). Further, GdmHCl titration of heat-treated hIgG4-Fc (Figure 6B) clearly demonstrates that unfolding

transitions are cooperative and that the heat-treated protein displays higher kinetic stability toward chemical denaturation than the native state. On the basis of these observations, we propose that the non-native structure of hIgG4-Fc formed upon heating should be termed an alternatively folded state rather than a molten globule. Thermal treatment results in the formation of protein oligomers (discussed below). Most probably, unfolding involves both dissociation of these oligomers and loss of structure within monomers, which may explain the apparently increased stability of the thermally induced structure compared to the monomeric native state; i.e., unfolding of the oligomers is kinetically controlled.

The alternatively folded state is often associated with the protein forming higher-order assemblies. AUC data reveal that hIgG4-Fc, after incubation at 75 °C for 10 min followed by re-equilibration at 25 °C, indeed exists as a mixture of different oligomeric structures in which the dominating equilibrium is that between the monomer and the heptamer. As discussed above, it is likely that solvent-exposed hydrophobic patches in the heat-treated protein are responsible for hydrophobic interchain interactions between individual hIgG4-Fc units, thus driving oligomerization. Interestingly, if hIgG4-Fc is heated for ≥30 min under quiescent conditions, it assembles into fibrous structures clearly visible in the TEM (Figure 7). Similar behavior has not been observed for the oligomer-forming antibody domains V_L, V_H, C_H1, and C_H3 under acidic conditions (*6*, *7*). The nature of the hIgG4-Fc fibers remains to be investigated.

This work was focused on the characterization of hIgG-Fc of subclass 4. Pronounced differences in far-UV CD spectra obtained from thermally denatured hIgG1-Fc, hIgG2-Fc, and hIgG3-Fc suggest that conclusions about the alternatively folded state as described in this report cannot be immediately generalized to the other subclasses. A detailed, subclass-wide structural analysis of thermal denaturation in hIgG-Fc will be important for understanding the determinants of formation of this state.

Although immunological implications of the alternatively folded state are not clear at this point, technical applications of heat-treated hIgG-Fc can be envisioned. For example, hIgG-Fc is an antigen for RF, a family of autoantibodies used as seromarkers for rheumatoid arthritis (*23*, *24*). Immunoassays for RF of the IgG isotype must be carefully designed, partly because its binding specificity overlaps with that of conventional detection antibodies. Interestingly, preliminary ELISA and SPR experiments have indicated that while Protein A binding capacity is abolished in heat-treated hIgG4-Fc, binding to IgG-RF is very similar with the two structural variants of the protein (unpublished data). In this way, heat-treated hIgG4-Fc can potentially be used as an antigen in *in vitro* assays for IgG-RF in combination with Protein A as the detection molecule.

In summary, we have shown that thermal denaturation of native hIgG4-Fc at pH 7.4 involves the formation of an alternatively folded state rather than a molten globule or a random structure. Alternatively folded states of other IgG fragments, as well as the full IgG, have previously been described only under acidic conditions. Our results thus expand the view of when all-β-sheet proteins can form this structural state. Intriguingly, hIgG4-Fc in the alternatively folded state forms fibrous structures in the micrometer range, and a characterization of these fibers with respect to the morphology and time scale of formation will be reported elsewhere.

ACKNOWLEDGMENT

We thank Dr. Sofie Nyström, Ms. Cecilia Andrésen, and Prof. Uno Carlsson for valuable discussions. D.K. is enrolled in the multidisciplinary graduate school Forum Scientium at Linköping University.

SUPPORTING INFORMATION AVAILABLE

AUC data with fitted curves. This material is available free of charge via the Internet at http://pubs.acs.org.

REFERENCES

1. Arai, M., and Kuwajima, K. (2000) Role of the molten globule state in protein folding. *Adv. Protein Chem. 53*, 209–282.
2. Buchner, J., Renner, M., Lilie, H., Hinz, H. J., Jaenicke, R., Kiefhaber, T., and Rudolph, R. (1991) Alternatively folded states of an immunoglobulin. *Biochemistry 30*, 6922–6929.
3. Welfle, K., Misselwitz, R., Hausdorf, G., Hohne, W., and Welfle, H. (1999) Conformation, pH-induced conformational changes, and thermal unfolding of anti-p24 (HIV-1) monoclonal antibody CB4-1 and its Fab and Fc fragments. *Biochim. Biophys. Acta 1431*, 120–131.
4. Lilie, H., and Buchner, J. (1995) Domain interactions stabilize the alternatively folded state of an antibody Fab fragment. *FEBS Lett. 362*, 43–46.
5. Buchner, J., Rudolph, R., and Lilie, H. (2002) Intradomain disulfide bonds impede formation of the alternatively folded state of antibody chains. *J. Mol. Biol. 318*, 829–836.
6. Thies, M. J. W., Kammermeier, R., Richter, K., and Buchner, J. (2001) The alternatively folded state of the antibody C(H)3 domain. *J. Mol. Biol. 309*, 1077–1085.
7. Feige, M. J., Simpson, E. R., Herold, E. M., Bepperling, A., Heger, K., and Buchner, J. (2010) Dissecting the alternatively folded state of the antibody Fab fragment. *J. Mol. Biol. 399*, 719–730.
8. Nozaki, Y. (1972) The preparation of guanidine hydrochloride. *Methods Enzymol. 26*, 43–50.
9. Greenfield, N. J. (2004) Analysis of circular dichroism data. *Methods Enzymol. 383*, 282–317.
10. Sreerama, N., and Woody, R. W. (2004) Computation and analysis of protein circular dichroism spectra. *Methods Enzymol. 383*, 318–351.
11. Semisotnov, G. V., Rodionova, N. A., Razgulyaev, O. I., Uversky, V. N., Gripas, A. F., and Gilmanshin, R. I. (1991) Study of the "molten globule" intermediate state in protein folding by a hydrophobic fluorescent probe. *Biopolymers 31*, 119–128.
12. Yang, J. J., Yang, H. D., Ye, Y. M., Hopkins, H., and Hastings, G. (2002) Temperature-induced formation of a non-native intermediate state of the all β-sheet protein CD2. *Cell Biochem. Biophys. 36*, 1–18.
13. Narhi, L. O., Philo, J. S., Li, T. S., Zhang, M., Samal, B., and Arakawa, T. (1996) Induction of α-helix in the β-sheet protein tumor necrosis factor-α: Thermal- and trifluoroethanol-induced denaturation at neutral pH. *Biochemistry 35*, 11447–11453.
14. Roychaudhuri, R., Sarath, G., Zeece, M., and Markwell, J. (2003) Reversible denaturation of the soybean Kunitz trypsin inhibitor. *Arch. Biochem. Biophys. 412*, 20–26.
15. Feige, M. J., Hendershot, L. M., and Buchner, J. (2010) How antibodies fold. *Trends Biochem. Sci. 35*, 189–198.
16. Ionescu, R. M., Vlasak, J., Price, C., and Kirchmeier, M. (2008) Contribution of variable domains to the stability of humanized IgG1 monoclonal antibodies. *J. Pharm. Sci. 97*, 1414–1426.
17. Tischenko, V. M., Abramov, V. M., and Zav'yalov, V. P. (1998) Investigation of the cooperative structure of Fc fragments from myeloma immunoglobulin G. *Biochemistry 37*, 5576–5581.
18. Souillac, P. O. (2005) Biophysical characterization of insoluble aggregates of a multi-domain protein: An insight into the role of the various domains. *J. Pharm. Sci. 94*, 2069–2083.
19. Mimura, Y., Church, S., Ghirlando, R., Ashton, P. R., Dong, S., Goodall, M., Lund, J., and Jefferis, R. (2000) The influence of glycosylation on the thermal stability and effector function expression of human IgG1-Fc: Properties of a series of truncated glycoforms. *Mol. Immunol. 37*, 697–706.
20. Vonderviszt, F., Lakatos, S., Gal, P., Sarvari, M., and Zavodszky, P. (1987) A molten globule-like unfolding intermediate of a four domain protein, the Fc fragment of the IgG molecule. *Biochem. Biophys. Res. Commun. 148*, 92–98.
21. Cowgill, R. W. (1967) Fluorescence and protein structure. XI. Fluorescence quenching by disulfide and sulfhydryl groups. *Biochim. Biophys. Acta 140*, 37–44.

22. Corper, A. L., Sohi, M. K., Bonagura, V. R., Steinitz, M., Jefferis, R., Feinstein, A., Beale, D., Taussig, M. J., and Sutton, B. J. (1997) Structure of human IgM rheumatoid factor Fab bound to its autoantigen IgG Fc reveals a novel topology of antibody-antigen interaction. *Nat. Struct. Biol. 4*, 374–381.
23. Renaudineau, Y., Jamin, C., Saraux, A., and Youinou, P. (2005) Rheumatoid factor on a daily basis. *Autoimmunity 38*, 11–16.
24. Mierau, R., and Genth, E. (2006) Diagnosis and prognosis of early rheumatoid arthritis, with special emphasis on laboratory analysis. *Clin. Chem. Lab. Med. 44*, 138–143.